Published by Institute of Physics Publishing for SISSA/ISAS

Received: *July 2, 2003*
Revised: *October 13, 2003*
Accepted: *October 30, 2003*

The shapes of Dirichlet defects

Mark Bowick, Antonio De Felice and Mark Trodden

Department of Physics, Syracuse University
Syracuse, NY 13244-1130, U.S.A.
E-mail: bowick@physics.syr.edu, defelice@physics.syr.edu, trodden@physics.syr.edu

Abstract: If the vacuum manifold of a field theory has the appropriate topological structure, the theory admits topological structures analogous to the D-branes of string theory, in which defects of one dimension terminate on other defects of higher dimension. The shapes of such defects are analyzed numerically, with special attention paid to the intersection regions. Walls (co-dimension 1 branes) terminating on other walls, global strings (co-dimension 2 branes) and local strings (including gauge fields) terminating on walls are all considered. Connections to supersymmetric field theories, string theory and condensed matter systems are pointed out.

Keywords: Solitons Monopoles and Instantons, Spontaneous Symmetry Breaking.

JHEP10(2003)067

Contents

1. Introduction **1**

2. Walls ending on walls **2**
2.1 The model 2
2.2 The numerical problem — boundary conditions 4
2.3 Results — walls on Dirichlet walls 5

3. Global strings ending on walls **6**
3.1 The model 6
3.2 The numerical problem — boundary conditions 7
3.3 Results — global strings ending on Dirichlet walls 8

4. Gauge strings on walls **9**
4.1 The model 9
4.2 The numerical problem — boundary conditions 11
4.3 Results — local strings ending on Dirichlet walls 12

A. Numerical details **14**

1. Introduction

Topological defects arise whenever spontaneous symmetry breaking leads to a topologically nontrivial manifold of vacua or ground states. Defect configurations involving spatially nonuniform order fields are of considerable interest in any field theory which possesses them as their topological quantum numbers distinguish them from vacua with uniform order fields. A complete understanding of the physical significance of defects requires a good knowledge of their field and energy profile and much effort has been devoted over the years to this subject (see [1, 2] for reviews). Applications range all the way from fundamental physics to cosmology and condensed matter phase transitions.

For a symmetry breaking phase transition $G \to H$, the vacuum manifold is given by the coset space $\mathcal{M} = G/H$, and p-dimensional defects are classified by the homotopy group $\pi_{d-p-1}(\mathcal{M})$, where d is the spatial dimensionality. For field theories with a relatively simple field content and abelian homotopy groups the associated topological defects are essentially isolated fundamental objects — they do not intersection

In more complicated field theories new possibilities arise involving composite defects or intersecting arrays of defects. Such configurations add a new layer of mathematical and physical richness. The simplest examples are p-dimensional defects whose boundaries are themselves $(p-1)$-dimensional defects [3]–[6]. Another example is furnished by theories with non-abelian homotopy groups, such as the quaternionic fundamental group of RP^2, in which topological defects of a fixed dimension (strings) intersection Some time ago Carroll and Trodden [7, 8] considered the case of defects which terminate when they intersect defects of equal or higher dimensionality, such as strings $(p = 1)$ ending on domain walls $(p = 2)$. The defects on which other defects end were termed *Dirichlet topological defects* (DTD), in analogy with D-branes in string theory [9]–[14], extended objects on which fundamental strings can terminate. It is important, of course, to keep in mind that there are important differences between the two sets of objects, as emphasized in [7, 15].

Related configurations are of interest in several contexts. Strings terminating on walls can arise in Yang-Mills theories [18]–[21] as well as in grand unified models, where they may be of use in tackling the monopole problem [16, 17]. In nonabelian gauge theories, non-intercommuting cosmic strings provide a further example. In addition, in higher spatial dimensions, the required symmetry breaking schemes can lead to a nonabelian unbroken gauge group, and the phenomenon of confinement for the resulting defects. The rich variety of symmetry breakings and associated ground state manifolds in condensed matter systems provides a particularly concrete context to study topological defects, including the Dirichlet class studied here. In fact an $N = 1$ vortex filament in the nonchiral superfluid ^{3}He-B phase can terminate at a domain wall interface separating this phase from a superfluid ^{3}He-A phase [22], thus realizing a string terminating on a wall.

Since interesting nonlinearities arise both in the cores of such defects and at the points at which distinct classes of defects intersect, it is important to have explicit solutions at hand to study, rather than simply a classification of the associated vacuum structure which guarantees their existence. Some work along these lines has already been performed, particularly in the case of defects networks in supersymmetric theories[1] [28]–[31] (for related work in the context of D-branes see [32]–[36]). This is the focus of the current paper, whose outline is now provided. In section 2 we treat the case of walls ending on walls, followed in section 3 by the case of global strings ending on walls. In section 4 we add gauge fields and treat the case of local strings terminating on walls. In each case we give explicit field and energy profiles. Throughout this paper we work in three spatial dimensions.

2. Walls ending on walls

2.1 The model

The simplest example of a DTD is a wall ending on another wall. Walls are produced by the spontaneous breaking of discrete symmetries. Consider a theory with three fields, ϕ, ψ_1 and ψ_2, invariant under three Z_2 symmetries. Such configurations are a special case of Z_n walls [37], and are related to solutions in supersymmetric [38, 39, 40] and

[1]For microphysical properties of defects in supersymmetric theories see [23]–[27].

supergravity [41, 42] theories.

$$
\begin{aligned}
&Z_2^{(1)} : (\phi \ \mapsto -\phi,\ \psi_1 \leftrightarrow \psi_2) \\
&Z_2^{(2)} :\ \psi_1 \mapsto -\psi_1 \\
&Z_2^{(3)} :\ \psi_2 \mapsto -\psi_2\,,
\end{aligned} \tag{2.1}
$$

with lagrangian density [7]

$$
\mathcal{L} = \frac{1}{2}\,\partial_\mu\phi\,\partial^\mu\phi + \frac{1}{2}\,\partial_\mu\psi_1\,\partial^\mu\psi_1 + \frac{1}{2}\,\partial_\mu\psi_2\,\partial^\mu\psi_2 - V(\phi,\psi_1,\psi_2)\,, \tag{2.2}
$$

where we choose the most general renormalizable potential invariant under $Z_2^{(1)}\times Z_2^{(2)}\times Z_2^{(3)}$

$$
V(\phi,\psi_1,\psi_2) = \lambda_\phi(\phi^2-\tilde{v}^2)^2 + \lambda_\psi\,[\psi_1^2+\psi_2^2-\tilde{w}^2+g(\phi^2-\tilde{v}^2)]^2 + h\psi_1^2\psi_2^2 - \mu\phi(\psi_1^2-\psi_2^2)\,. \tag{2.3}
$$

For $\mu = 0$, the minima of V are the 8 points given by

$$
\phi = \pm\tilde{v} \qquad \text{and} \qquad \begin{cases} (\psi_1,\psi_2) = (\pm\tilde{w},0) \\ \text{or} \\ (\psi_1,\psi_2) = (0,\pm\tilde{w})\,. \end{cases} \tag{2.4}
$$

Since the potential is positive-definite in this case, the presence of h requires either ψ_1 or ψ_2 to vanish, after which the first term in the potential is minimized by $\phi = \pm\tilde{v}$ and the second term by $\psi_1 = \pm\tilde{w}$ or $\psi_2 = \pm\tilde{w}$. For $\mu > 0$ the degeneracy of the 8 vacua is broken, leaving only 4 minima of the potential, at

$$
\phi = v, \qquad (\psi_1,\psi_2) = (\pm w, 0)\,; \tag{2.5}
$$

$$
\phi = -\,v, \qquad (\psi_1,\psi_2) = (0,\pm w)\,, \tag{2.6}
$$

where v is the solution of the cubic equation

$$
8\lambda_\phi\lambda_\psi\,v^3 + 6\lambda_\psi g\mu\,v^2 - (8\lambda_\phi\lambda_\psi\tilde{v}^2 + \mu^2)\,v - 2\lambda_\psi\mu\,(g\tilde{v}^2+\tilde{w}^2) = 0\,, \tag{2.7}
$$

satisfying $\lim_{\mu\to 0} v = \tilde{v}$, and w is given by

$$
w = \left[\tilde{w}^2 + g(\tilde{v}^2 - v^2) + \frac{\mu v}{2\lambda_\psi}\right]^{1/2}. \tag{2.8}
$$

The equations of motion for static fields are then

$$
\nabla^2\phi \ = 4\lambda_\phi\phi(\phi^2-\tilde{v}^2) + 4g\lambda_\psi\phi[\psi_1^2+\psi_2^2-\tilde{w}^2+g(\phi^2-\tilde{v}^2)] - \mu(\psi_1^2-\psi_2^2) \tag{2.9}
$$

$$
\nabla^2\psi_1 = 4\lambda_\psi\psi_1[\psi_1^2+\psi_2^2-\tilde{w}^2+g(\phi^2-\tilde{v}^2)] + 2h\psi_1\psi_2^2 - 2\mu\phi\psi_1 \tag{2.10}
$$

$$
\nabla^2\psi_2 = 4\lambda_\psi\psi_2[\psi_1^2+\psi_2^2-\tilde{w}^2+g(\phi^2-\tilde{v}^2)] + 2h\psi_1^2\psi_2 + 2\mu\phi\psi_2\,. \tag{2.11}
$$

This model is constructed to admit solutions consisting of domain walls terminating on other domain walls. Such a configuration is intrinsically two-dimensional, and hence is independent of one spatial coordinate, which we choose to be z. What remains is a boundary value problem for an elliptic system of partial differential equations, for which we must prescribe the value of the fields on the boundary.

2.2 The numerical problem — boundary conditions

Our choice of boundary conditions is illustrated in figure 1,[2] so that we have Dirichlet boundary conditions

$$\begin{aligned} \phi(x, y = -\infty) &= -v\,, \\ \psi_1(x, y = -\infty) &= 0\,, \\ \psi_2(x, y = -\infty) &= w\,, \end{aligned} \tag{2.12}$$

at $y \to -\infty$, and Neumann boundary conditions everywhere else except at the upper corners, at which we choose

$$\begin{aligned} \phi(x = \pm\infty, y = +\infty) &= v\,, \\ \psi_1(x = \pm\infty, y = +\infty) &= \pm w\,, \\ \psi_2(x = \pm\infty, y = +\infty) &= 0\,. \end{aligned} \tag{2.13}$$

These choices define a wall in the ψ_1 field, terminating on a wall in the ϕ field — the Dirichlet wall.

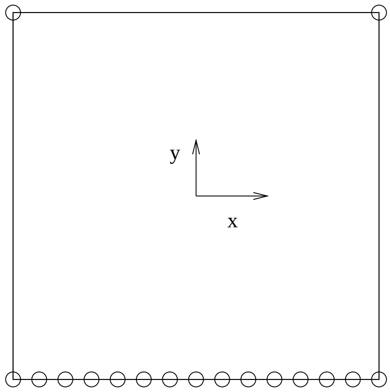

Figure 1: Boundary conditions for walls on walls. The circles ($\circ$) represent Dirichlet boundary conditions and solid lines represents Neumann boundary conditions.

The numerical algorithms we use require homogeneous boundary conditions and so we introduce new fields

$$\begin{aligned} \phi\; &= u_0 + F_0\,, \\ \psi_1 &= u_1 + F_1\,, \\ \psi_2 &= u_2 + F_2\,, \end{aligned} \tag{2.14}$$

and define

$$\begin{aligned} F_0(x,y) &= f_{0s}(y) + \frac{1+\tanh(2y)}{2}\left[f_{0u}(x) - f_{0s}(y=+\infty)\right], \\ F_1(x,y) &= f_{1s}(y)\tanh(2x) + \frac{1+\tanh(2y)}{2}\left[f_{1u}(x) - f_{1s}(y=+\infty)\tanh(2x)\right], \\ F_2(x,y) &= f_{2s}(y)\,. \end{aligned} \tag{2.15}$$

The functions $f_{iu}(x)$ and $f_{is}(y)$ are the solutions of the systems of ordinary differential equations obtained by restricting (2.9)–(2.11) to the "up" boundary ($y = +\infty$) and the "side" boundary ($x = +\infty$) respectively, with $i = 0, 1, 2$ corresponding to ϕ, ψ_1, ψ_2 respectively.

These functions are easily found using standard algorithms with boundary conditions

$$\begin{aligned} f_{0u}(\pm\infty) &= v\,, \\ f_{1u}(\pm\infty) &= \pm w\,, \\ f_{2u}(\pm\infty) &= 0\,. \end{aligned} \tag{2.16}$$

$$\begin{aligned} f_{0s}(-\infty) &= -v & f_{0s}(+\infty) &= v \\ f_{1s}(-\infty) &= 0 & f_{1s}(+\infty) &= w \\ f_{2s}(-\infty) &= w & f_{2s}(+\infty) &= 0\,. \end{aligned} \tag{2.17}$$

[2]Higher resolution figures are available at: `http://www.physics.syr.edu/~defelice/dirichlet.html`.

JHEP10(2003)067

The symmetries of our problem are such that the solutions on the boundary at $x = -\infty$ are then $\psi_1(x = -\infty, y) = -f_{1s}(y)$ and $\psi_2(x = -\infty, y) = f_{2s}(y)$. Note that one solution $f_{2u}(x) \equiv 0$ is trivial.

We are now in a position to solve numerically our partial differential equations in the interior. We use a multigrid algorithm [43] to solve for the fields u_i, satisfying

$$\begin{aligned} u_i &= 0 \qquad \text{at the } y = -\infty \text{ boundary and at } (x, y) = (\pm\infty, +\infty)\ , \\ \partial_x u_i &= 0 \qquad \text{at } x = \pm\infty\,, \\ \partial_y u_i &= 0 \qquad \text{at } y = +\infty\,. \end{aligned} \tag{2.18}$$

2.3 Results — walls on Dirichlet walls

We present our results as a set of plots of field profiles and energy densities, providing a number of ways of viewing configuration shapes. We have already defined the field profiles, and the energy density for static fields is given by

$$\begin{aligned} E = {T^0}_0 = -\mathcal{L} = \frac{1}{2}\left(\frac{\partial\phi}{\partial x}\right)^2 + \frac{1}{2}\left(\frac{\partial\phi}{\partial y}\right)^2 + \frac{1}{2}\left(\frac{\partial\psi_1}{\partial x}\right)^2 + \frac{1}{2}\left(\frac{\partial\psi_1}{\partial y}\right)^2 + \\ + \frac{1}{2}\left(\frac{\partial\psi_2}{\partial x}\right)^2 + \frac{1}{2}\left(\frac{\partial\psi_2}{\partial y}\right)^2 + V(\phi, \psi_1, \psi_2)\,. \end{aligned} \tag{2.19}$$

The ϕ field domain wall configuration is plotted in figure 2. The intersection with the ψ_1 wall at $x = 0$ is clearly visible. The corresponding configuration for ψ_1 is shown in figure 3. Note the domain wall for $y = +\infty$. Finally the ψ_2 field configuration is plotted in figure 4. It has the form of a wall with half the height of the Dirichlet wall in the sense that it goes from 0 (at $y = +\infty$) to $w = 1$ (at $y = -\infty$). The energy density plotted in figure 5 illustrates the merging of the walls at the origin. A corresponding contour plot for the energy density in figure 6 shows the wall merging very clearly.

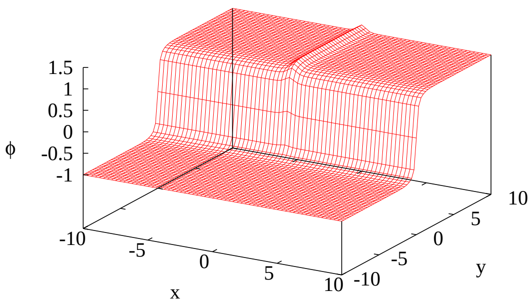

Figure 2: The ϕ Dirichlet wall configuration.

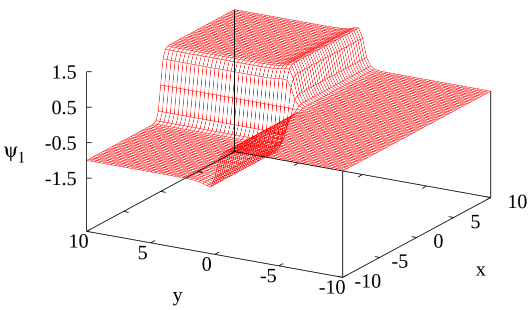

Figure 3: Field configuration for ψ_1.

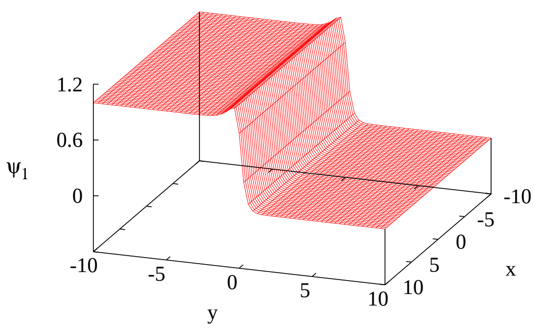

Figure 4: Walls on walls field configuration for ψ_2.

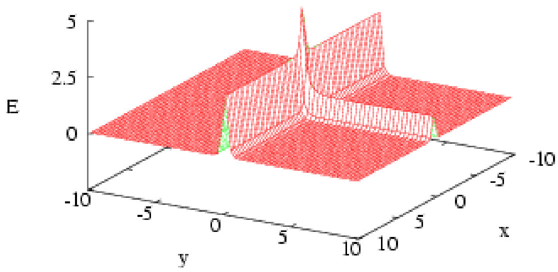

Figure 5: Energy density for walls ending on walls.

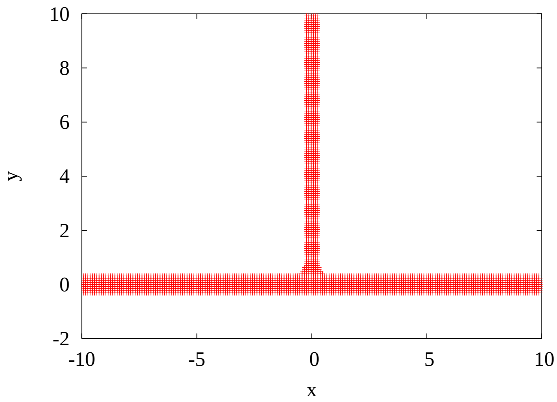

Figure 6: Contour plot of the energy density for walls ending on walls.

3. Global strings ending on walls

3.1 The model

In the simplest case, strings are generated by a breakdown of a U(1) symmetry. In analogy with our approach in the previous section, consider the following transformations on one real scalar field ϕ and two complex scalar fields ψ_1 and ψ_2.

$$\begin{aligned} Z_2 :&\ \ (\phi \mapsto -\phi, \psi_1 \leftrightarrow \psi_2) \\ \mathrm{U}(1)_1 :&\ \ \psi_1 \mapsto \mathrm{e}^{-i\omega_1}\, \psi_1 \\ \mathrm{U}(1)_2 :&\ \ \psi_2 \mapsto \mathrm{e}^{-i\omega_2}\, \psi_2\,. \end{aligned} \tag{3.1}$$

In this section, both U(1) symmetries are global, i.e. ω_i is space-time independent. The lagrangian density is

$$\mathcal{L} = \frac{1}{2}\,\partial_\mu\phi\,\partial^\mu\phi + \partial_\mu\bar{\psi}_1\,\partial^\mu\psi_1 + \partial_\mu\bar{\psi}_2\,\partial^\mu\psi_2 - V(\phi,\psi_1,\psi_2)\,, \tag{3.2}$$

with potential

$$\begin{aligned} V(\phi,\psi_1,\psi_2) = {}& \lambda_\phi(\phi^2-\tilde{v}^2)^2 + \lambda_\psi\left[|\psi_1|^2+|\psi_2|^2-\tilde{w}^2+g(\phi^2-\tilde{v}^2)\right]^2 + \\ & + h|\psi_1|^2|\psi_2|^2 - \mu\phi(|\psi_1|^2-|\psi_2|^2)\,. \end{aligned} \tag{3.3}$$

Consider the following static ansatz

$$\begin{aligned} \phi &= \phi(r,z) \\ \psi_1 &= R_1(r,z)\,e^{i\theta} \\ \psi_2 &= \psi_2(r,z)\,, \end{aligned} \tag{3.4}$$

where ϕ, R_1 and ψ_2 are real functions, for which the equations of motion are

$$\nabla^2\phi = 4\lambda_\phi\phi(\phi^2-\tilde{v}^2) + 4\lambda_\psi g\phi[R_1^2+\psi_2^2-\tilde{w}^2+g(\phi^2-\tilde{v}^2)] - \mu(R_1^2-\psi_2^2)\,, \tag{3.5}$$

$$\nabla^2 R_1 = 2\lambda_\psi R_1\,[R_1^2+\psi_2^2-\tilde{w}^2+g(\phi^2-\tilde{v}^2)] + hR_1\psi_2^2 - \mu\phi R_1\,, \tag{3.6}$$

$$\nabla^2\psi_2 = 2\lambda_\psi\psi_2\,[R_1^2+\psi_2^2-\tilde{w}^2+g(\phi^2-\tilde{v}^2)] + hR_1^2\psi_2 + \mu\phi\psi_2\,. \tag{3.7}$$

JHEP10(2003)067

3.2 The numerical problem — boundary conditions

We now proceed as in the previous section, imposing the boundary conditions illustrated in figure 7.

We choose Dirichlet boundary conditions for the bottom boundary

$$\begin{aligned} \phi(r, z=-\infty) &= -v\,, \\ R_1(r, z=-\infty) &= 0\,, \\ \psi_2(r, z=-\infty) &= w\,, \end{aligned} \tag{3.8}$$

and at the upper corner we impose

$$\begin{aligned} \phi(r=\infty,\, z=+\infty) &= v\,, \\ R_1(r=\infty,\, z=+\infty) &= w\,, \\ \psi_2(r=\infty,\, z=+\infty) &= 0\,. \end{aligned} \tag{3.9}$$

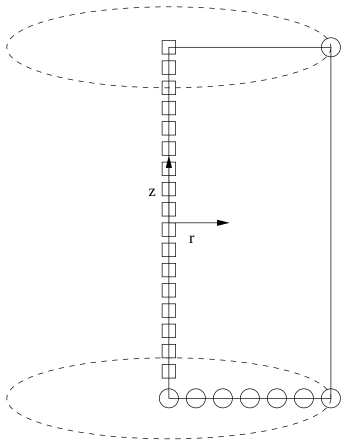

Figure 7: Boundary conditions for a string ending on a wall. The circles (○) represent Dirichlet boundary conditions, the squares (□) represent mixed boundary conditions (Dirichlet for some fields, Neumann for the remaining ones) and solid lines represent Neumann boundary conditions.

The boundary $r = 0$ requires a more detailed discussion. Taylor expanding the fields around $r = 0$, we have

$$\phi = \sum_n a_n(z)\, r^n\,, \qquad R_1 = \sum_n b_n(z)\, r^n\,, \qquad \psi_2 = \sum_n c_n(z)\, r^n\,. \tag{3.10}$$

Equations (3.5)–(3.7), in the limit $r \to 0$, become

$$\begin{aligned} \frac{a_1(z)}{r} + 4a_2(z) + \frac{d^2 a_0(z)}{dz^2} &= f_0[a_0(z), b_0(z), c_0(z)]\,, \\ 3b_2(z) - \frac{b_0(z)}{r^2} + \frac{d^2 b_0(z)}{dz^2} &= f_1[a_0(z), b_0(z), c_0(z)]\,, \\ \frac{c_1(z)}{r} + 4c_2(z) + \frac{d^2 c_0(z)}{dz^2} &= f_2[a_0(z), b_0(z), c_0(z)]\,. \end{aligned} \tag{3.11}$$

Demanding regularity at the origin gives

$$\begin{aligned} a_1(z) &= 0 \qquad & \partial_r\phi|_{r=0} &= 0\,, \\ b_0(z) &= 0 \qquad & R_1|_{r=0} &= 0\,, \\ c_1(z) &= 0 \qquad & \partial_r\psi_2|_{r=0} &= 0\,. \end{aligned} \tag{3.12}$$

For the other boundaries we imposed Neumann boundary conditions for all the fields.

As for the case of walls on walls, we define new fields with homogeneous boundary conditions. Defining the "up" boundary to be at $z = +\infty$ and the "side" boundary to be at $r = +\infty$ we again introduce the functions $f_{iu}(r)$ and $f_{is}(z)$ which are solutions to the appropriate systems of ordinary differential equations with boundary conditions

$$\begin{aligned}
\partial_r f_{0u}(0) &= 0 \qquad & f_{0u}(+\infty) &= v\,, \\
f_{1u}(0) &= 0 \qquad & f_{1u}(+\infty) &= w\,, \\
\partial_r f_{2u}(0) &= 0 \qquad & f_{2u}(+\infty) &= 0\,,
\end{aligned} \tag{3.13}$$

$$\begin{aligned}
f_{0s}(-\infty) &= -v \qquad & f_{0s}(+\infty) &= v\,, \\
f_{1s}(-\infty) &= \ 0 \qquad & f_{1s}(+\infty) &= w\,, \\
f_{2s}(-\infty) &= \ w \qquad & f_{2s}(+\infty) &= 0\,.
\end{aligned} \tag{3.14}$$

Again we have a trivial solution $f_{2u}(r) \equiv 0$. Following the previous section, we define the following functions

$$\begin{aligned}
F_0(r,z) &= f_{0s}(z) + \frac{1+\tanh(2z)}{2}\left[f_{0u}(r) - f_{0s}(z=+\infty)\right], \\
F_1(r,z) &= f_{1s}(z)\tanh(r) + \frac{1+\tanh(2z)}{2}\left[f_{1u}(r) - f_{1s}(z=+\infty)\tanh(r)\right], \quad F_2(r,z) = f_{2s}(z)\,,
\end{aligned}$$

and introduce new fields

$$\begin{aligned}
\phi &= u_0 + F_0\,, \\
\psi_1 &= u_1 + F_1\,, \\
\psi_2 &= u_2 + F_2\,,
\end{aligned} \tag{3.15}$$

obeying homogeneous boundary conditions

$$\begin{aligned}
u_i &= 0 \qquad && \text{at the } z=-\infty \text{ boundary, at } (r,z) = (+\infty,+\infty) \\
& && \text{and for } u_1 \text{ at the core of the string,} \\
\partial_r u_i &= 0 \qquad && \text{at the } r=+\infty \text{ boundary and for } i=0,2 \text{ at the core of the string,} \\
\partial_z u_i &= 0 \qquad && \text{at the } z=+\infty \text{ boundary}.
\end{aligned}$$

3.3 Results — global strings ending on Dirichlet walls

To help in understanding our plots, note that the energy density for static fields in this section is given by

$$\begin{aligned}
E = T^0{}_0 = -\mathcal{L} &= \frac{1}{2}\left(\frac{\partial\phi}{\partial r}\right)^2 + \frac{1}{2}\left(\frac{\partial\phi}{\partial z}\right)^2 + \left(\frac{\partial\psi_2}{\partial r}\right)^2 + \left(\frac{\partial\psi_2}{\partial z}\right)^2 + \\
&\quad + \left(\frac{\partial R_1}{\partial r}\right)^2 + \frac{R_1^2}{r^2} + \left(\frac{\partial R_1}{\partial z}\right)^2 + V(\phi, R_1, \psi_2)\,.
\end{aligned} \tag{3.16}$$

The ϕ field domain wall configuration is plotted in figure 8. The intersection with the ψ_1 string at $r=0$ is clearly visible. The corresponding configuration for ψ_1 is shown in figure 9. Note the string for $z=+\infty$. Finally the ψ_2 field configuration is plotted in

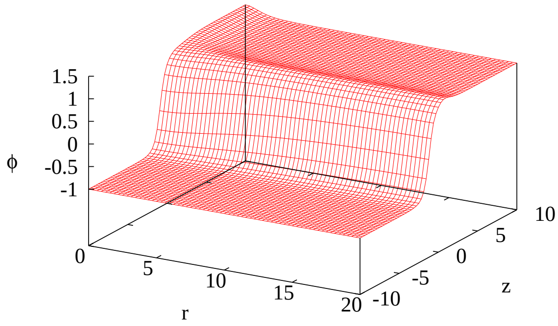

Figure 8: Field ϕ, the Dirichlet wall.

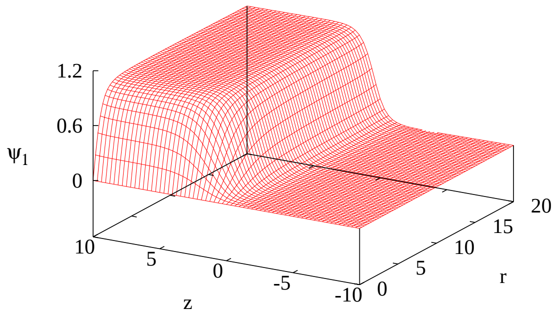

Figure 9: Field ψ_1, the global string.

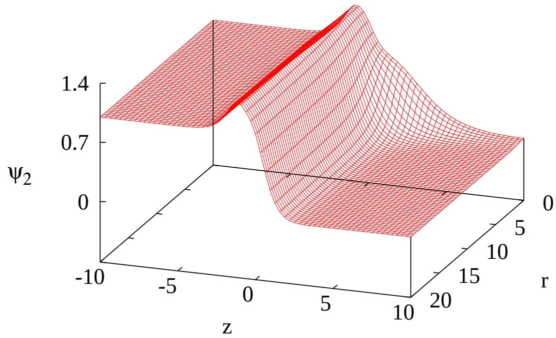

Figure 10: Field ψ_2 for a global string and a wall.

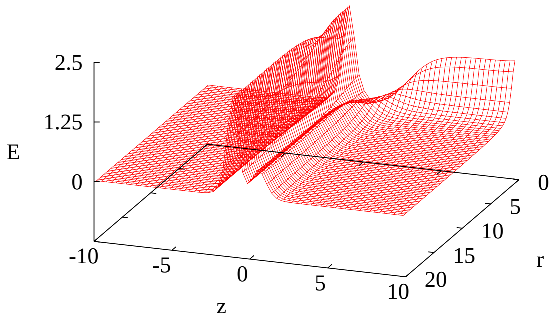

Figure 11: Energy density for a global string ending on a wall.

figure 10. It has the form of a wall (except for an interaction with the string for $r = 0$ and $z > 0$) with half the height of the Dirichlet wall in the sense that it goes from 0 (at $z = +\infty$) to $w = 1$ (at $z = -\infty$).

The energy density plotted in figure 11 illustrates the merging of the string with the wall at the origin. A corresponding contour plot for the energy density in figure 12 shows the string ending on the wall very clearly.

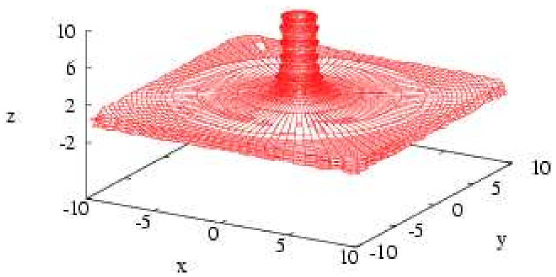

Figure 12: Contour plot of the energy density for a global string ending on a wall.

4. Gauge strings on walls

More interesting connections with physical models can be made by introducing gauge fields. In this section we take the first steps towards this by finding numerical solutions for local cosmic strings terminating on Dirichlet domain walls.

4.1 The model

We modify the lagrangian density of the last section by introducing a U(1) gauge field A_μ, under which the field ψ_1 is charged.

$$\mathcal{L} = \frac{1}{2}\,\partial_\mu\phi\,\partial^\mu\phi + \bar{D}_\mu\bar{\psi}_1\,D^\mu\psi_1 + \partial_\mu\bar{\psi}_2\,\partial^\mu\psi_2 - \frac{1}{4}\,F^{\mu\nu}F_{\mu\nu} - V(\phi,\psi_1,\psi_2)\,, \tag{4.1}$$

where

$$D_\mu = \partial_\mu - ieA_\mu\,. \tag{4.2}$$

The equations of motion for ϕ and ψ_2 are unchanged from the case of the global string, since we have constructed the model so that the relevant winding occurs for the ψ_1 field only. Thus, the modified equation of motion for ψ_1 is

$$\partial_\mu\partial^\mu\psi_1 - ie\partial_\mu(A^\mu\psi_1) + \frac{\partial V}{\partial\bar{\psi}_1} - ieA_\mu(\partial^\mu\psi_1 - ieA^\mu\psi_1) = 0\,. \tag{4.3}$$

Imposing the Lorentz condition $\partial_\mu A^\mu = 0$ for a static gauge field yields

$$\vec{\nabla}\cdot\vec{A} = 0\,, \tag{4.4}$$

and equation (4.3) then becomes

$$\nabla^2\psi_1 = \frac{\partial V}{\partial\bar{\psi}_1} - 2ie\vec{A}\cdot\vec{\nabla}\psi_1 + e^2(\vec{A}\cdot\vec{A})\psi_1\,. \tag{4.5}$$

We are interested in the ansatz

$$\begin{aligned}
\phi\ &= \phi(r,z)\,,\\
\psi_1 &= R_1(r,z)\,e^{i\theta}\,,\\
\psi_2 &= \psi_2(r,z)\,,
\end{aligned} \tag{4.6}$$

where ϕ, R_1 and ψ_2 are real functions. As is well known for cosmic strings, the imaginary part of equation (4.5) gives

$$A_r\,\frac{\partial R_1}{\partial r} + A_z\,\frac{\partial R_1}{\partial z} = 0\,, \tag{4.7}$$

with solution

$$\vec{A} = A\,\hat{\theta}\,, \tag{4.8}$$

so that the Lorentz condition becomes $\partial_\theta A = 0$. The equation for R_1 then becomes

$$\begin{aligned}
\nabla^2 R_1 &= \frac{\partial^2 R_1}{\partial r^2} + \frac{1}{r}\,\frac{\partial R}{\partial r} - \frac{R_1}{r^2} + \frac{\partial^2 R_1}{\partial z^2}\\
&= 2\lambda_\psi R_1\,[R_1^2 + \psi_2^2 - \tilde{w}^2 + g(\phi^2 - \tilde{v}^2)] + hR_1\psi_2^2 - \mu\phi R_1 + 2e\,\frac{AR_1}{r} + e^2A^2R_1\,,
\end{aligned} \tag{4.9}$$

and the equation for the gauge field is

$$\Box A^\alpha = j^\alpha = 2e\,\mathrm{Im}[\bar{\psi}_1(\partial^\alpha - ieA^\alpha)\psi_1]\,, \tag{4.10}$$

which, for our ansatz, is

$$(\vec{\nabla}^2\vec{A})_\theta = 2e\,R_1^2\,(r^{-1} + eA)\,. \tag{4.11}$$

4.2 The numerical problem — boundary conditions

The geometry of the problem is identical to that for global strings, and so we refer the reader again to figure 7. We choose Dirichlet boundary conditions for the bottom boundary

$$\begin{aligned}\phi(r, z=-\infty) &= -v\,,\\ R_1(r, z=-\infty) &= 0\,,\\ \psi_2(r, y=-\infty) &= w\,,\\ A(r, y=-\infty) &= 0\,,\end{aligned} \tag{4.12}$$

and at the upper corner

$$\begin{aligned}\phi(r=\infty, z=+\infty) &= v\,,\\ R_1(r=\infty, z=+\infty) &= w\,,\\ \psi_2(r=\infty, z=+\infty) &= 0\,,\\ A(r=\infty, z=+\infty) &= 0\,.\end{aligned} \tag{4.13}$$

At the core of the string we choose

$$\begin{aligned}\partial_r\phi(r=0, z) = \partial_r\psi_2(r=0, z) &= 0\,,\\ R_1(r=0, z) = A(r=0, z) &= 0\,,\end{aligned} \tag{4.14}$$

and for the boundary at $r = +\infty$ we impose Neumann conditions for all the fields. The choice of these boundary conditions defines a string ending on a Dirichlet wall.

We again solve ordinary differential equations on the boundaries at $z = +\infty$ and $r = +\infty$. We keep the same notation as in the previous section, but now include the gauge field A by defining $f_{3u}(r)$ and $f_{3s}(z)$ with boundary conditions

$$\begin{aligned}f_{3u}(0) &= 0 \qquad & \partial_r f_{3u}(+\infty) &= 0\,,\\ f_{3s}(-\infty) &= 0 \qquad & f_{3s}(+\infty) &= 0\,.\end{aligned} \tag{4.15}$$

Once again $f_{2u}(r) \equiv 0$ and $f_{3s}(z) \equiv 0$ are trivial solutions.

As before we define

$$\begin{aligned}F_0(r,z) &= f_{0s}(z) + \frac{1+\tanh(2z)}{2}\,[f_{0u}(r) - f_{0s}(z=+\infty)]\,,\\ F_1(r,z) &= f_{1s}(z)\tanh(r) + \frac{1+\tanh(2z)}{2}\,[f_{1u}(r) - f_{1s}(z=+\infty)\tanh(r)]\,,\\ F_2(r,z) &= f_{2s}(z)\,,\\ F_3(r,z) &= \frac{1+\tanh(2z)}{2}\,f_{3u}(r)\,,\end{aligned} \tag{4.16}$$

and new fields

$$\begin{aligned}\phi &= u_0 + F_0\,,\\ \psi_1 &= u_1 + F_1\,,\\ \psi_2 &= u_2 + F_2\,,\\ A &= u_3 + F_3\,,\end{aligned} \tag{4.17}$$

JHEP10(2003)067

with homogeneous boundary conditions

$$\begin{aligned}
u_i = 0 \qquad & \text{at the } z = -\infty \text{ boundary, at the corner } (r, z) = (+\infty, +\infty) \\
& \text{and, for } i = 1, 3, \text{ at the core of the string,} \\
\partial_r u_i = 0 \qquad & \text{at the } r = +\infty \text{ boundary and, for } i = 0, 2, \text{ at the core of the string,} \\
\partial_z u_i = 0 \qquad & \text{at the } z = +\infty \text{ boundary}\,.
\end{aligned}$$

4.3 Results — local strings ending on Dirichlet walls

We plot our results as before, with the energy density now given by

$$E = {T^0}_0 = -\mathcal{L} = \frac{1}{2}\left(\frac{\partial\phi}{\partial r}\right)^2 + \frac{1}{2}\left(\frac{\partial\phi}{\partial z}\right)^2 + \left(\frac{\partial\psi_2}{\partial r}\right)^2 + \left(\frac{\partial\psi_2}{\partial z}\right)^2 + \\ + \left(\frac{\partial R_1}{\partial r}\right)^2 + R_1^2\left(\frac{1}{r} + eA\right)^2 + \left(\frac{\partial R_1}{\partial z}\right)^2 + \frac{1}{2}\vec{B}^2 + V(\phi, R_1, \psi_2)\,. \tag{4.18}$$

We also plot the magnetic field associated with the gauge field of the string, given by

$$\vec{B} = -\frac{\partial A}{\partial z}\,\hat{r} + \frac{1}{r}\frac{\partial(rA)}{\partial r}\,\hat{z}\,. \tag{4.19}$$

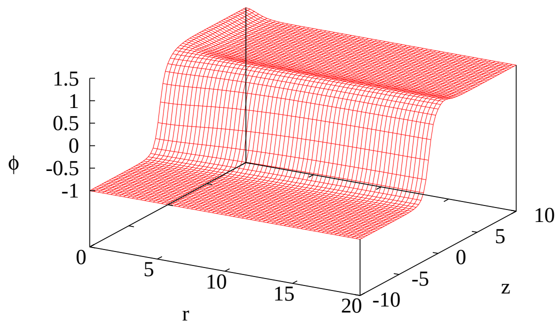

Figure 13: The ϕ field configuration: Dirichlet wall for local strings.

The ϕ field domain wall configuration is plotted in figure 13. The intersection with the ψ_1 string at $r = 0$ is clearly visible. The corresponding configuration for ψ_1 is shown in figure 14. Note the string for $z = +\infty$. The field ψ_2 configuration is plotted in figure 15. It has the form of a wall (except for an interaction with the string for $r = 0$ and $z > 0$) with half the height of the Dirichlet wall in the sense that it goes from 0 (at $z = +\infty$) to $w = 1$ (at $z = -\infty$). Finally the gauge field configuration is shown in figure 16. We can verify that $A \to r^{-1}$ as $(r, z) \to +\infty$. We plotted the r component of the magnetic field, B_r, in figure 17. The z component of the magnetic field, B_z, is illustrated in figure 18. A 2-D plot of the vector field $\vec{B}$ is

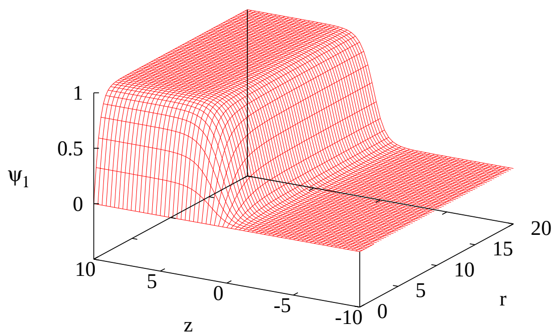

Figure 14: The local string field ψ_1.

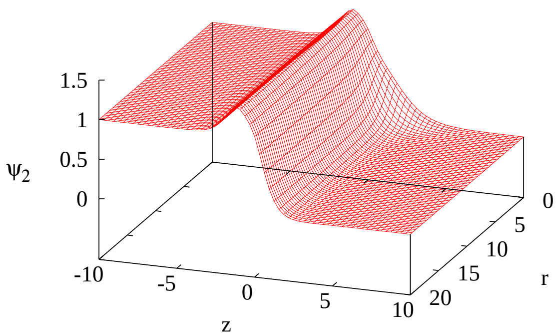

Figure 15: Field configuration ψ_2 for a local string ending on a wall.

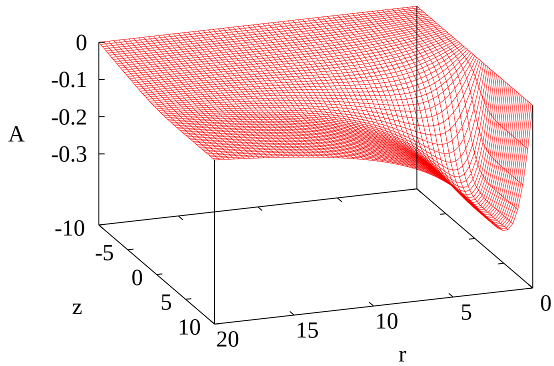

Figure 16: The gauge field A.

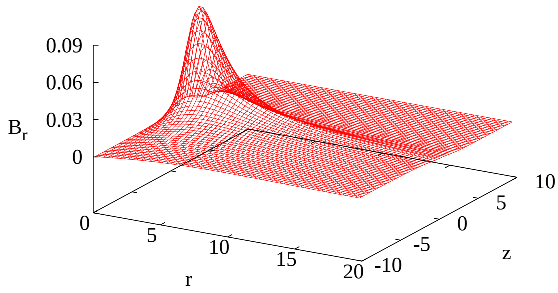

Figure 17: Component B_r of the magnetic field.

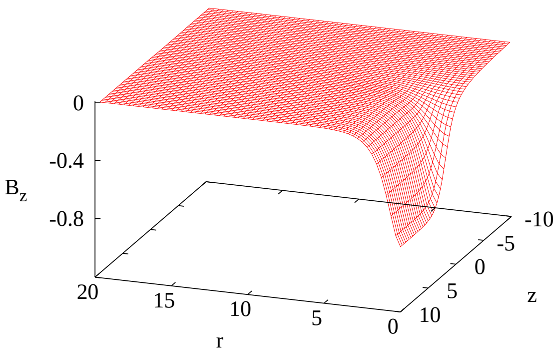

Figure 18: Component B_z of the magnetic field.

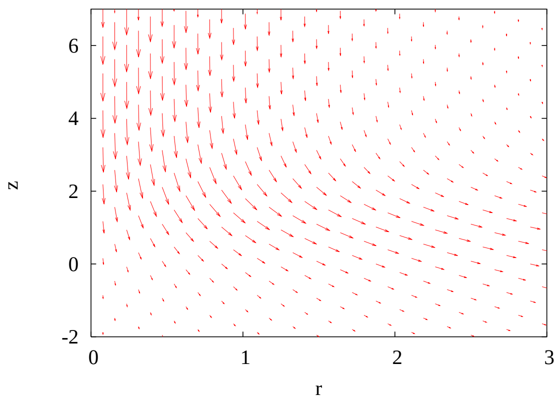

Figure 19: 2D plot of the magnetic field $\vec{B}$.

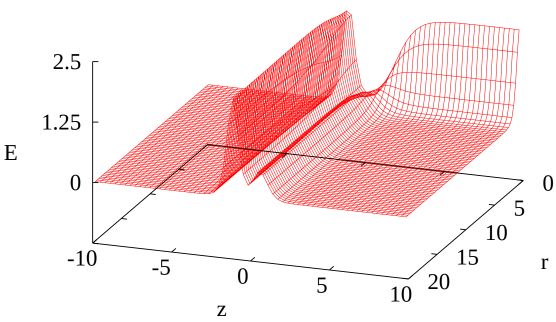

Figure 20: Energy density for a local string ending on a wall.

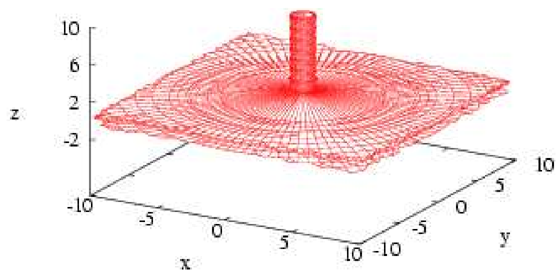

Figure 21: Contour plot for the energy density for a local string ending on a wall.

shown in figure 19. The energy density plotted in figure 20 illustrates the string merging at the origin with the Dirichlet wall. A corresponding contour plot of the energy density in figure 21 shows the string ending on the wall very clearly.

Acknowledgments

We thank Joel Rozowsky for helpful discussions. M.B. is supported by the US Department of Energy (DOE) under contract No. DE-FG02-85ER40237 and by the National Science Foundation (NSF) under grant DMR-0219292. A.D.F. and M.T. are supported in part by the NSF under grant PHY-0094122. M.T. is a Cottrell Scholar of Research Corporation.

A. Numerical details

The defect solutions described in this paper were obtained by directly solving the appropriate set of elliptical partial differential equations, together with prescribed boundary values, as opposed to minimizing the associated energy functional. The differential equations were solved by writing our own C++ code employing two distinct algorithms: a *multigrid* algorithm for boundary value problems and a *successive overrelaxation* (SOR) algorithm. C implementations of both these algorithms may be found in [44]. In our case we had to deal with both Dirichlet and Neumann boundary conditions, as opposed to the purely Dirichlet boundary conditions treated in [44].

All the free parameters in our equations were set to one except for the coupling constant μ, which was usually taken to vanish. We checked that our results were qualitatively unchanged for non-zero μ. We were also careful to choose a sufficiently large domain for the solutions to have the expected asymptotic behavior at infinity. To be precise we chose $-10 \leq x \leq 10$ and $-10 \leq y \leq 10$ for the walls whereas $0 \leq r \leq 20$ and $-10 \leq z \leq 10$ for the strings.

We used grids with 257, 513 and 1025 points. For the 513 point grid the numerical solutions required 8 hours total computational time on a PC Pentium 4.

References

[1] A. Vilenkin and E.P.S. Shellard, *Cosmic strings and other topological defects*, Cambridge University Press, Cambridge 1994.

[2] M.B. Hindmarsh and T.W.B. Kibble, *Cosmic strings*, *Rept. Prog. Phys.* **58** (1995) 477 [hep-ph/9411342].

[3] T.W.B. Kibble, G. Lazarides and Q. Shafi, *Walls bounded by strings*, *Phys. Rev.* **D 26** (1982) 435.

[4] A. Vilenkin, *Cosmological evolution of monopoles connected by strings*, *Nucl. Phys.* **B 196** (1982) 240.

[5] M. Hindmarsh and T.W.B. Kibble, *Beads on strings*, *Phys. Rev. Lett.* **55** (1985) 2398.

[6] A. Chamblin and D.M. Eardley, *Puncture of gravitating domain walls*, *Phys. Lett.* **B 475** (2000) 46 [hep-th/9912166].

[7] S.M. Carroll and M. Trodden, *Dirichlet topological defects*, *Phys. Rev.* **D 57** (1998) 5189 [hep-th/9711099].

[8] M. Trodden, *Dirichlet solitons in field theories*, hep-th/9901062.

[9] P. Hořava, *Strings on world sheet orbifolds*, *Nucl. Phys.* **B 327** (1989) 461.

[10] P. Hořava, *Background duality of open string models*, *Phys. Lett.* **B 231** (1989) 251.

[11] J. Dai, R.G. Leigh and J. Polchinski, *New connections between string theories*, *Mod. Phys. Lett.* **A 4** (1989) 2073.

[12] J. Polchinski, *Dirichlet-branes and Ramond-Ramond charges*, *Phys. Rev. Lett.* **75** (1995) 4724 [hep-th/9510017].

[13] J. Polchinski, S. Chaudhuri and C.V. Johnson, *Notes on D-branes*, hep-th/9602052.

[14] J. Polchinski, *Lectures on D-branes*, hep-th/9611050.

[15] G. Dvali and A. Vilenkin, *Solitonic D-branes and brane annihilation*, *Phys. Rev.* **D 67** (2003) 046002 [hep-th/0209217].

[16] G.R. Dvali, H. Liu and T. Vachaspati, *Sweeping away the monopole problem*, *Phys. Rev. Lett.* **80** (1998) 2281 [hep-ph/9710301].

[17] S. Alexander, R.H. Brandenberger, R. Easther and A. Sornborger, *On the interaction of monopoles and domain walls*, hep-ph/9903254.

[18] E. Witten, *Branes and the dynamics of QCD*, *Nucl. Phys.* **B 507** (1997) 658 [hep-th/9706109].

[19] A. Campos, K. Holland and U.J. Wiese, *Complete wetting in supersymmetric QCD or why QCD strings can end on domain walls*, *Phys. Rev. Lett.* **81** (1998) 2420 [hep-th/9805086].

[20] K. Holland and U.-J. Wiese, *The center symmetry and its spontaneous breakdown at high temperatures*, hep-ph/0011193.

[21] G.R. Dvali, G. Gabadadze and Z. Kakushadze, *BPS domain walls in large-N supersymmetric QCD*, *Nucl. Phys.* **B 562** (1999) 158 [hep-th/9901032].

[22] G.E. Volovik, *Monopoles and fractional vortices in chiral superconductors*, *Proc. Nat. Acad. Sci.* **97** (2000) 2431 [cond-mat/9911486].

[23] S.C. Davis, A.-C. Davis and M. Trodden, *$N = 1$ supersymmetric cosmic strings*, *Phys. Lett.* **B 405** (1997) 257 [hep-ph/9702360].

[24] S.C. Davis, A.C. Davis and M. Trodden, *Cosmic strings, zero modes and SUSY breaking in nonabelian $N = 1$ gauge theories*, *Phys. Rev.* **D 57** (1998) 5184 [hep-ph/9711313].

[25] J.R. Morris, *Superconducting domain walls from a supersymmetric action*, *Phys. Rev.* **D 52** (1995) 1096.

[26] J.R. Morris, *Supersymmetry and gauge invariance constraints in a $\mathrm{U}(1) \times \mathrm{U}(1)'$-Higgs superconducting cosmic string model*, *Phys. Rev.* **D 53** (1996) 2078 [hep-ph/9511293].

[27] J.R. Morris, *Cosmic strings in supergravity*, *Phys. Rev.* **D 56** (1997) 2378 [hep-ph/9706302].

[28] D. Bazeia, H. Boschi-Filho and F.A. Brito, *Domain defects in systems of two real scalar fields*, *J. High Energy Phys.* **04** (1999) 028 [hep-th/9811084].

[29] P.M. Saffin, *Tiling with almost-BPS-invariant domain-wall junctions*, *Phys. Rev. Lett.* **83** (1999) 4249 [hep-th/9907066].

[30] D. Bazeia and F.A. Brito, *Bags, junctions and networks of BPS and non-BPS defects*, *Phys. Rev.* **D 61** (2000) 105019 [hep-th/9912015].

[31] D. Bazeia, F.A. Brito, W. Freire and R.F. Ribeiro, *Confining potential in a color dielectric medium with parallel domain walls*, hep-th/0210289.

JHEP10(2003)067

[32] E. Witten, *Solutions of four-dimensional field theories via M-theory*, *Nucl. Phys.* **B 500** (1997) 3 [hep-th/9703166].

[33] C.G. Callan Jr. and J.M. Maldacena, *Brane dynamics from the Born-Infeld action*, *Nucl. Phys.* **B 513** (1998) 198 [hep-th/9708147].

[34] G.W. Gibbons, *Born-Infeld particles and Dirichlet p-branes*, *Nucl. Phys.* **B 514** (1998) 603 [hep-th/9709027].

[35] P.S. Howe, N.D. Lambert and P.C. West, *The self-dual string soliton*, *Nucl. Phys.* **B 515** (1998) 203 [hep-th/9709014].

[36] A. Hashimoto, *The shape of branes pulled by strings*, *Phys. Rev.* **D 57** (1998) 6441 [hep-th/9711097].

[37] B.S. Ryden, W.H. Press and D.N. Spergel, *The evolution of networks of domain walls and cosmic strings*, *Astrophys. J.* **357** (1990) 293.

[38] G.W. Gibbons and P.K. Townsend, *A Bogomol'nyi equation for intersecting domain walls*, *Phys. Rev. Lett.* **83** (1999) 1727 [hep-th/9905196].

[39] S.M. Carroll, S. Hellerman and M. Trodden, *Domain wall junctions are 1/4-BPS states*, *Phys. Rev.* **D 61** (2000) 065001 [hep-th/9905217].

[40] J.P. Gauntlett, R. Portugues, D. Tong and P.K. Townsend, *D-brane solitons in supersymmetric sigma-models*, *Phys. Rev.* **D 63** (2001) 085002 [hep-th/0008221].

[41] S.M. Carroll, S. Hellerman and M. Trodden, *BPS domain wall junctions in infinitely large extra dimensions*, *Phys. Rev.* **D 62** (2000) 044049 [hep-th/9911083].

[42] A. Hashimoto, *Supergravity solutions for localized intersections of branes*, *J. High Energy Phys.* **01** (1999) 018 [hep-th/9812159].

[43] U. Trottenberg, C. Oosterlee and A. Schüller, *Multigrid*, Academic Press, San Diego 2001.

[44] See section 19 of W.H. Press, B.P. Flannery, S.A. Teukolsky and W.T. Vetterling, *Numerical recipes in C*, Cambridge University Press, Cambridge 1992; See also http://www.library.cornell.edu/nr/bookcpdf.html.

JHEP10(2003)067